Polymer 50 (2009) 3905–3910

Contents lists available at ScienceDirect

Polymer

journal homepage: www.elsevier.com/locate/polymer

Poly(methyl methacrylate)/clay nanocomposites by photoinitiated free radical polymerization using intercalated monomer

Ayhan Oral [a], Mehmet Atilla Tasdelen [b], Adem Levent Demirel [c], Yusuf Yagci [b,*]

[a] Department of Chemistry, Faculty of Sciences and Arts, Canakkale Onsekiz Mart University, 17020, Canakkale, Turkey
[b] Department of Chemistry, Istanbul Technical University, 34469, Maslak, Istanbul, Turkey
[c] Chemistry Department, Koc University, Rumelifeneri Yolu, 34450, Sariyer, Istanbul, Turkey

ARTICLE INFO

Article history:
Received 14 May 2009
Accepted 8 June 2009
Available online 12 June 2009

Keywords:
Nanocomposites
Click chemistry
Poly(methyl methacrylate)

ABSTRACT

A series of poly(methyl methacrylate)/montmorillonite (PMMA/MMT) nanocomposite were prepared by successfully dispersing the inorganic nanolayers of MMT clay in an organic PMMA matrix via *in situ* photoinitiated free radical polymerization. Methyl methacrylate monomer was first intercalated into the interlayer regions of organophilic clay hosts by "click" chemistry followed by a typical photoinitiated free radical polymerization. The intercalated monomer was characterized by FT-IR spectroscopy, elemental analysis and thermogravimetric analysis methods. The intercalation ability of the modified monomer and exfoliated nanocomposite structure were confirmed by X-ray diffraction spectroscopy (XRD), transmission electron microscopy (TEM) and atomic force microscopy (AFM). Thermal stability of PMMA/MMT nanocomposites was also studied by both differential scanning calorimetry (DSC) and thermogravimetric analysis (TGA).

1. Introduction

Polymer/clay nanocomposites have received a great deal of attention in both academia and industry because of their enhanced physical properties. For example, thermal, and flammability properties are all improved relative to the virgin polymer [1]. Three methods have been developed over time for the preparation of polymer/clay nanocomposites: (1) solution exfoliation, (2) melt intercalation and (3) *in situ* polymerization [2–4]. Among them, *in situ* polymerization technique, involving intercalation of the monomer, initiator and/or catalyst within the silicate layers is the most common method. The polymerization is then initiated by external stimulation such as thermal, photochemical or chemical activation [5–8]. *In situ* photoinitiated free radical polymerization has many obvious advantages compared to thermal polymerization, including low temperature conditions, solvent-free formulation and a rapid polymerization rate.

The poly(methyl methacrylate) (PMMA) is completely amorphous, and has high strength, outstanding outdoor weathering properties, good optical transparency and excellent dimensional stability due to rigid polymer chains [9]. These properties of PMMA provide significant importance for biomedical material, dental, and surgical applications, and an important engineering material for electronics, optical communication. The thermal and thermomechanical properties of PMMA can be improved by addition of a small amount of montmorillonite nanolayers.

In recent years, "click chemistry", the copper (I) catalyzed Huisgen's azide-alkyne [3 + 2] cycloaddition reaction, has been received tremendous attention because of its quantitative yield, short reaction time, applicability under mild reaction conditions and a high tolerance toward other functional groups [10–12]. This methodology has been subsequently expanded in macromolecular engineering [13–22], surface modification [23] of both nanoparticles [24,25] and silica [26,27], functionalization of carbon nanotubes [28]. We have recently applied this chemistry for the exfoliation through the functional groups of the intercalant that readily react with the antagonist groups of the preformed polymers (Scheme 1). In this manner, polymer/clay nanocomposites were successfully prepared by "click" chemistry [27].

In this study, we report the preparation of PMMA/clay nanocomposite via *in situ* photoinitiated polymerization. The method consists of the intercalation of methyl methacrylate monomer into silicate layers by "click chemistry" and followed by *in situ* photopolymerization of mixing intercalated and virgin monomer. Polymerization of methyl methacrylate in the silicate layers leads to polymer/clay nanocomposites which are formed by individually dispersing inorganic silica nanolayers in the polymer matrix.

* Corresponding author. Tel.: +90 212 285 3241; fax: +90 212 285 6386.
E-mail address: yusuf@itu.edu.tr (Y. Yagci).

0032-3861/$ – see front matter © 2009 Elsevier Ltd. All rights reserved.
doi:10.1016/j.polymer.2009.06.020

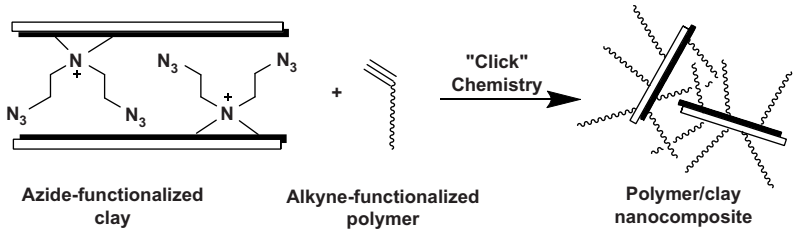

Scheme 1. Preparation of polymer/clay nanocomposites by "click" chemistry.

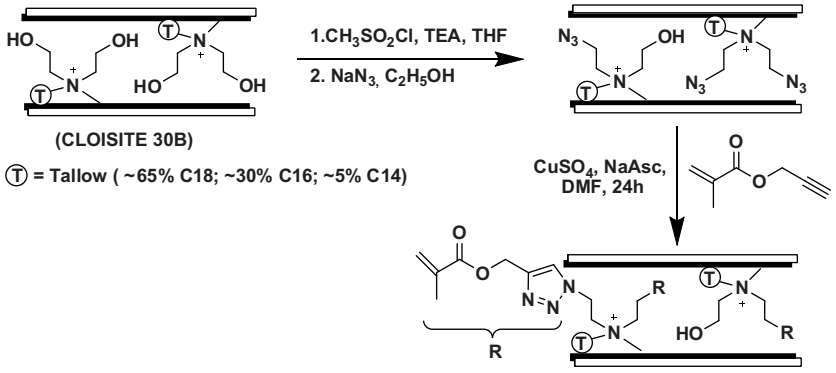

Scheme 2. Synthesis of azide-functionalized montmorillonite clay and its "click" reaction with propargyl methacrylate.

2. Experimental

2.1. Materials

Azide-functionalized montmorillonite clay (MMT-N_3) [27] and propargyl methacrylate [29] were synthesized as described previously. Organically modified clay, Cloisite 30B, was purchased from Southern Clay products, Gonzales, TX, USA. The organic content of the organo-modified montmorillonite, determined by TGA, was 21 wt%. Before use, the clay was dried under vacuum at 110 °C for 1 h. Methyl methacrylate (MMA, 99%, Aldrich) was passed through basic alumina column to remove the inhibitor. Benzoin (Bz, 98%, Aldrich) was recrystallized from ethanol. Other solvents and chemicals were purified by conventional drying and distillation procedures. Tetrahydrofuran (THF; Aldrich HPLC grade) was dried on sodium wire under reflux in the presence of traces of benzophenone until a blue color persisted and was used directly after distillation. Dichloromethane (Acros HPLC grade) was stored on calcium hydride and used after distillation. Triethylamine (Aldrich, HPLC grade) were purified by distillation just before use. Sodium azide (NaN_3, Acros 99%), copper(II)sulfate.$5H_2O$ ($CuSO_4$, Acros 99%), L-ascorbic acid sodium salt (NaAsc, Acros 99%), methanesulfonyl chloride (Acros 99.5%), lithium bromide (LiBr, Fluka 98%), propargyl alcohol (Aldrich, 99%), propargyl methacrylate (Lancaster, 98%), dimethyl sulfoxide (DMSO, Acros HPLC grade), methanol (Acros HPLC grade) and ethanol (Acros 96%) were used as received.

2.2. Characterization

FT-IR spectra were recorded on a Perkin–Elmer FT-IR Spectrum One B spectrometer. Thermal gravimetric analysis (TGA) was performed on Perkin–Elmer Diamond TA/TGA with a heating rate of 10 °C × min under nitrogen flow. Elemental analyses were obtained from Thermo Finnigan Flash 1112. X-ray diffraction (XRD) patterns were obtained with a Japanese Rigaku D/max X-ray diffractometer equipped with graphite-monochromatized Cu K radiation ($\lambda = 1.54$ Å). Bragg's law ($\lambda = 2d\sin\theta$) was used to calculate the basal spacing (d_{001}) of clay layers. Transmission electron microscopy (TEM) analysis was performed using Philips-FEI Tecnai G2 F20 S-Twin 120 kV accelerating voltage. The samples have been dispersed in chloroform and then, some drops were deposited on a carbon supporting grid. After solvent evaporation, the TEM micrograph analyses were performed. For atomic force microscopy (AFM) measurements, thin films were spin coated from 10 mg/mL solutions in chloroform on silicon substrates. NT-MDT Solver P47 atomic force microscopy (AFM) was used in tapping mode for morphological characterization. Ultrasharp Si cantilevers having force constant of 48 N/m were used.

2.3. Synthesis of azide-functionalized montmorillonite clay (MMT-N_3)

Methyl bis(2-hydroxyethyl) (tallow alkyl) ammonium-organo-modified clay (MMT-$(CH_2CH_2OH)_2$, 4.50 g, 5.3 mmol, OH content)

Table 1
Properties of clays calculated by elemental, thermogravimetric, XRD and FT-IR analyses.

Sample	C (wt%)	H (wt%)	N (wt%)	Total[a] (wt%)	Total[b] (wt%)	d_{001}[c] (nm)	FT-IR %T (cm^{-1})
MMT-$(CH_2CH_2OH)_2$	18.53	3.15	1.27	23.0	21	1.77	OH(3410), C–H(3000), Si–O–Si(1040)
MMT-$(CH_2CH_2N_3)_2$	18.65	3.01	1.60	23.3	22	1.79	OH(3410), C–H(3000), N_3(2040), Si–O–Si(1040)
MMT-$(CH_2CH_2$-MA$)_2$	18.90	3.20	1.74	23.9	25	1.82	OH(3410), C–H(3000), C=O(1730), C=C(1635), Si–O–Si(1040)

[a] Calculated by elemental analysis.
[b] Calculated by thermogravimetric analysis.
[c] Basal spacing (d_{001}) is calculated by XRD analysis.

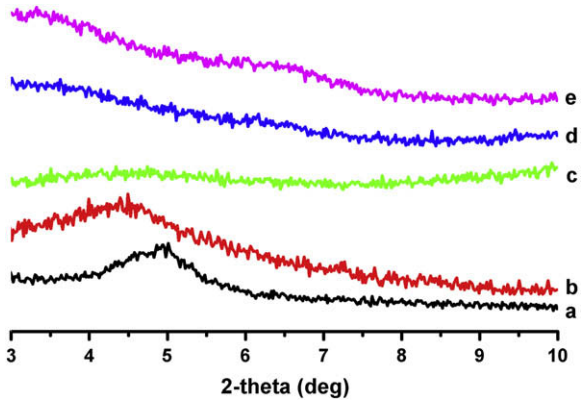

Fig. 1. X-ray diffraction of commercial clay (a), methyl methacrylate anchored clay (b), % 1 (c), % 3 (d) and % 5 (e) clay loaded nanocomposites.

and triethylamine (3.7 mL, 26.5 mmol) were added in THF (200 mL) and cooled to 0 °C. Methanesulfonyl chloride (2.1 mL, 26.5 mmol) was added drop wise while stirring. The reaction mixture was allowed to heat up to room temperature and stirred overnight. Solvent was removed by rotary evaporation, and ethanol (200 mL) was added to the reaction mixture. Sodium azide (1.72 g, 26.5 mmol) was added, and the reaction mixture was refluxed overnight. After cooling to room temperature and removing the solvent by rotary evaporation, ether (200 mL) was added to the crude reaction mixture and washed three times with a saturated NaCl aqueous solution. The clay was then filtered off on a cold glass filter, washed with water, and finally dried in vacuum.

2.4. Preparation of intercalated monomer (I-MA) via "click" coupling reaction

Azide-MMT (0.5 g, 6 mmol), propargyl methacrylate (0.4 mL, 3 mmol), hydroquinone and DMSO (20 mL) were combined in round bottom flask and stirred under nitrogen atmosphere. A solution of $CuSO_4$ (0.02 g, 0.12 mmol) in 1 mL of water was added to the mixture followed by addition of a solution of sodium ascorbate (0.09 g, 0.45 mmol) in 1 mL water. The mixture was heated in an oil bath at 70 °C overnight. The particles were recovered by filtration and washed with excess of water. The particles were recovered by centrifugation at 3000 rpm for 30 min. Then they are redispersed in water, and the mixture was centrifuged; this cycle was repeated four times. Finally, resulting product was dried in a vacuum oven.

2.5. Preparation of the PMMA/clay nanocomposites

The intercalated monomer (1, 3, and 5% of the monomer by weight) and benzoin (1% of the monomer by weight) mixed with MMA (2 mL) monomer solution in bulk were put into a pyrex tube (i.d. 9 mm) that was flushed with dry nitrogen. The mixture was irradiated in a photoreactor (Rayonet) equipped with 16 lamps emitting light nominally at 300 nm at room temperature. The light intensity was measured as 3 mW cm^{-1} by Delta Ohm model HD-9021 radiometer. At the end of 1 h, polymers were precipitated into methanol and then dried under reduced pressure.

3. Results and discussion

In previous works, methacrylate or styrene functional quaternary ammonium salts were used with sodium montmorillonite clay to make intercalated monomer [30–36]. Exfoliated or intercalated polymer/clay nanocomposites were achieved by *in situ* polymerization using this intercalated monomer. In our case, to anchor the methacrylate monomer into the clay, we convert the hydroxyl functionality of commercial montmorillonite clay (Cloisite 30B) to azide functionality through reaction with methanesulfonyl chloride and sodium azide. The other click component, propargyl methacrylate was synthesized via esterification reaction between propargyl alcohol and methacryloyl chloride according to the literature method [29]. Finally, "click" reaction would proceed in the clay layers between azide-functionalized clay and propargyl methacrylate to obtain intercalated methacrylate monomer. The overall process is represented in Scheme 2.

FT-IR analysis confirmed the presence of the azide group in the clay intergalleries. In Table 1, the FT-IR data of modified clay shows azide band as a strong absorbance at 2040 cm^{-1}. However, the presence of a broadband at 3410 cm^{-1} indicates that small quantity of the hydroxyl groups on the surface of the layers remained unreacted. After the "click" reaction, the characteristic azide signal at 2040 cm^{-1} has disappeared and new signals near 1730 and 1635 cm^{-1} corresponding to the carbonyl and acrylate group of the methacrylate group have appeared. These FT-IR spectral observations are basically in good agreement with the successful "click" reaction.

Table 1 also summarizes the average chemical composition of each element (C, H and N) and basal spacing values of the clay at different stages. The values of organic content calculated from C, H and N contents were found to be reasonable and in the range of experimental error. The organic contents were also measured with thermogravimetric analysis (TGA). As can be seen from Table 1, both analyses confirm a slight increase in the organic content of commercial clay by the modification and click reaction. These results together with the spectral analysis indicate that methacrylate group was successfully fixed in the clay layers by click reaction. Another evidence for occurrence of the click reaction was obtained from XRD pattern shown in Fig. 1. The basal spacings (d_{001}) of commercial and modified clay layer were found to be 1.76 nm and 1.82 nm (Table 1). The increment of interlayer spacing indicates an intercalated system with insertion of monomer into clay layers.

Table 2
Photopolymerization[a] of methyl methacrylate in the presence of intercalated monomer and thermal properties of the resulting composites.

Samples	Clay (wt%)	Conv.[b] (%)	d_{001}[c] (nm)	T_g[d] (°C)	Weight loss temperature[e] (°C)		Char yield[e] (%)
					10 wt%	50 wt%	
NC-0	0	91	–	132.7	219	357	0.0
NC-1	1	68	–	134.8	296	360	3.0
NC-3	3	46	–	138.2	314	359	7.3
NC-5	5	40	2.65	141.2	320	360	12.5

[a] [Photoinitiator]:1% of the monomer by weight.
[b] Determined by gravimetrically.
[c] Basal spacing (d_{001}) is calculated by XRD analysis.
[d] Determined by DSC analysis.
[e] Determined by TGA analysis.

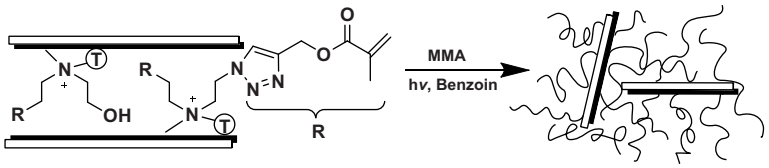

Scheme 3. Preparation of the PMMA/clay nanocomposites.

Thus, intercalated monomer was prepared by simple and quantitative "click" reaction under mild conditions, from cheap easily available reagents.

A series of PMMA/MMT nanocomposites was prepared by photoinitiated polymerization using different clay loadings and the results were collected in Table 2. The copolymerization of the intercalated monomer and purified methyl methacrylate could gradually push the layers apart, leading to delamination of clay tactoids (Scheme 3). A slight decrease on the monomer conversion was observed by increasing clay content. This effect could be due to that the presence of clay leads to a less efficient activation by the UV light or it someway interferes with the polymerization [37]. As it can be seen from Fig. 1, for the nanocomposites NC1, NC3 and NC5 exfoliated structures were obtained with absence of any d_{001} reflection in the XRD region. The increase of XRD intensity for NC3 and NC5 toward $2\theta \sim 3^{\circ}$ may be due to a broad peak resulting from partially exfoliated or intercalated structures as indicated by AFM measurements. According to literature, the amount of clay in the polymer is an important parameter for the clay layers to be close to one another [2]. From this point, the high clay content can lead to uncompleted exfoliation and intercalated structures.

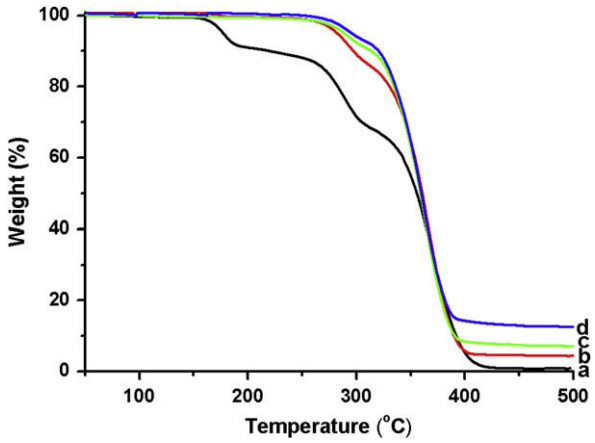

Fig. 2. Weight loss for pure PMMA (a) and PMMA nanocomposites containing 1 (b), 3 (c) and 5 (d), wt% clay.

Typical TGA curves for virgin PMMA and its nanocomposites are shown in Fig. 2 and the overall results are collected in Table 2. Hirata et al. reported that three main reaction stages take place during degradation of virgin PMMA under nitrogen [38]. These steps are head-to-head linkages, the range between 160 and 240 °C, end-chain saturation around 290 °C and the random scission of the polymer chains, the range between 300 and 400 °C. In Fig. 2, pure PMMA displays these three reaction stages, while the nanocomposites display only the second stage indicating random scission decomposition. The PMMA/clay nanocomposites exhibited higher decomposition temperatures than did virgin PMMA; that is the thermal stability of the nanocomposites was enhanced by the presence of dispersed clay nanolayers in accordance with the literature reports [39–43]. The PMMA/clay nanocomposites obviously have greater char yield, which increases upon increasing the clay content, as expected. The increase in char yield implies the reduction of the polymer's flammability. According to the DSC characterization, the T_g temperature of the nanocomposites increased with the clay content by a maximum of 8.5 °C.

The homogeneity of the dispersion of clay in the nanocomposites was determined by AFM measurements of spin coated thin films. Fig. 3 shows the AFM height images of NC-1, NC-3 and NC-5. All samples showed homogeneously dispersed regions of larger height on top of a smooth polymer film. These regions had different phase contrast than the polymer matrix indicating the presence of clay in them. With increasing clay content, the surface density of these regions also increased, as expected.

The common feature in all three samples was regions of height 5–10 nm whose shape varied between circular to rod like at the surface. This may reflect the various sizes and the orientations of the exfoliated clay sheets. The number of regions having larger height and lateral size also increased with the clay content which may be due to some partially exfoliated or intercalated structures in the system. Such structures were especially dominant for NC-5 in consistent with XRD and TGA measurements.

In addition to surface protrusions, higher magnification 2 μm × 2 μm AFM height and phase scans of the nanocomposite films also showed ~2 nm deep, 40–90 nm wide surface depressions in the smooth polymer matrix (Fig. 4). In the phase picture of NC-5 (Fig. 4f), a brighter phase contrast is clearly seen in these

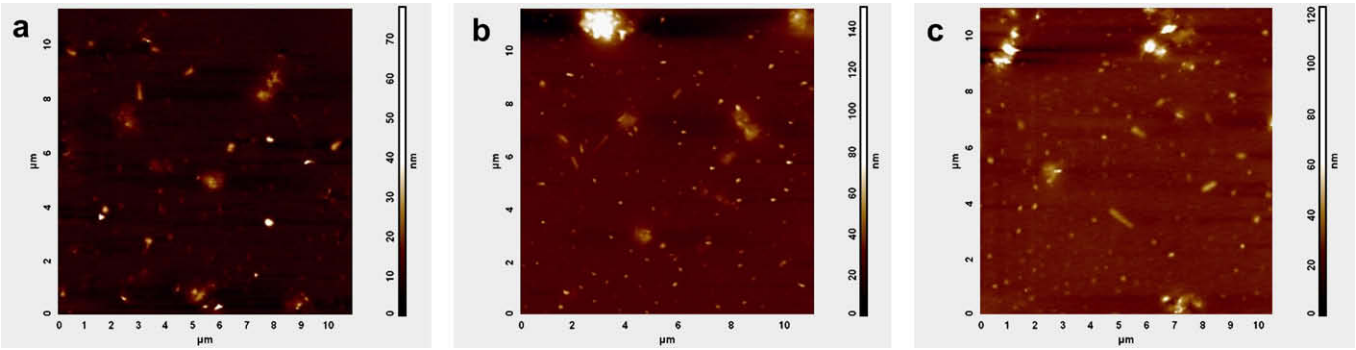

Fig. 3. 10 μm × 10 μm AFM height images of PMMA/clay nanocomposites: (a) NC-1; (b) NC-3; (c) NC-5.

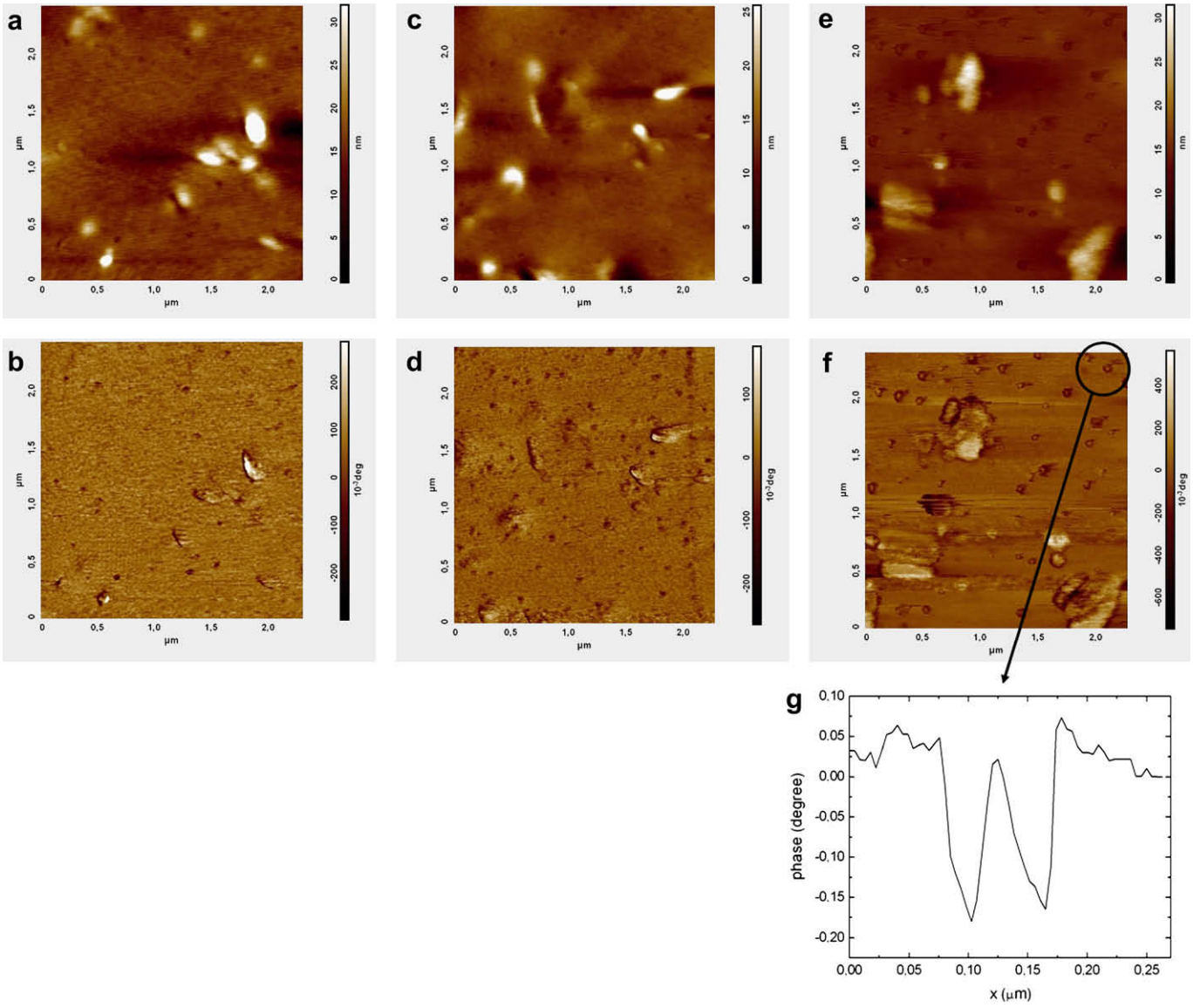

Fig. 4. 2 µm × 2 µm AFM height (top row) and phase (bottom row) images of PMMA/clay nanocomposites: (a, b) NC-1; (c, d) NC-3; (e, f) NC-5; (g) the phase profile of the encircled region in (f) along the *x*-axis.

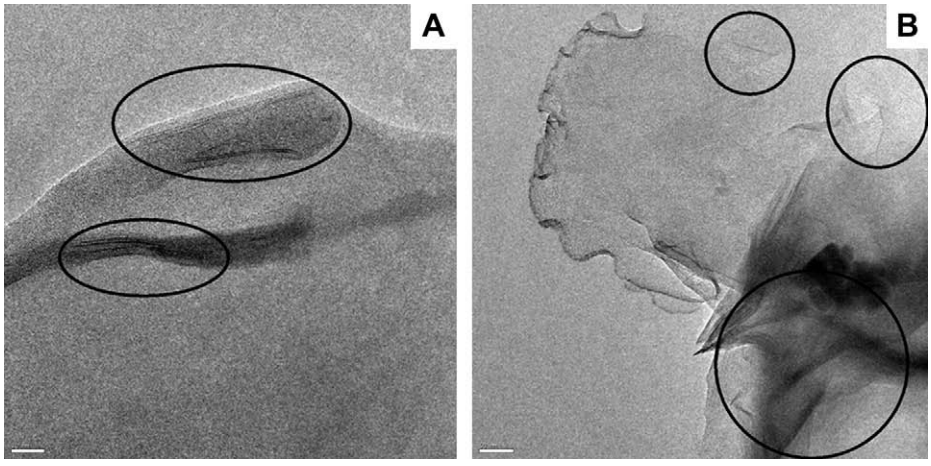

Fig. 5. TEM micrographs of PMMA/clay nanocomposites; intercalated (A) and exfoliated (B) structures.

depression regions. The phase profile along the *x*-axis through the depression in the upper right corner in Fig. 4f is plotted in Fig. 4g which indicates the presence of a harder phase in the depression. We attribute these regions also to exfoliated clay sheets lying just beneath the top surface of the polymer.

More information on the nanocomposite morphology is obtained by transmission electronic microscopy (TEM) observation as displayed in Fig. 5. Exfoliated silicate sheets (as highlighted by black circles) are observed together with small stacks of intercalated montmorillonite. This structure may be described as the incomplete activation of hydroxyl group in the polymerization due to the limited mobility of these groups within the layers.

4. Conclusions

Methacrylate-modified clay has been prepared by "click" chemistry and used to produce PMMA/clay nanocomposites by *in situ* photoinitiated free radical polymerization. Polymerization through the interlayer galleries of the clay was achieved by copolymerization of methyl methacrylate and intercalated monomer. The random dispersion of silicate layers in the polymer matrix was confirmed by XRD, AFM and TEM measurements. Exfoliation/intercalation structures were found to be related to the loading degree. TGA traces showed that the nanocomposites have higher thermal stabilities relative to that of the pristine PMMA. The char yields increased upon raising the clay content. This work and our previous report [6] clearly demonstrate that *in situ* photoinitiated free radical polymerization is an elegant way to prepare polymer/clay nanocomposites at room temperature through either incorporation chromophoric or olefinic groups as photoinitiator or polymerizable monomer, respectively into clay layers. The click chemistry approach presented here is not limited to the monomeric functional groups but it can also be applied to the incorporation of other various functional and polymeric structures. Further studies in this line are now in progress.

References

[1] Giannelis EP. Advanced Materials 1996;8(1):29–35.
[2] Ray SS, Okamoto M. Progress in Polymer Science 2003;28(11):1539–641.
[3] Alexandre M, Dubois P. Materials Science & Engineering R-Reports 2000; 28(1–2):1–63.
[4] Okamoto M. Materials Science and Technology 2006;22(7):756–79.
[5] Akat H, Tasdelen MA, Du Prez F, Yagci Y. European Polymer Journal 2008;44(7):1949–54.
[6] Nese A, Sen S, Tasdelen MA, Nugay N, Yagci Y. Macromolecular Chemistry and Physics 2006;207(9):820–6.
[7] Oral A, Tasdelen MA, Demirel AL, Yagci Y. Journal of Polymer Science, Part A: Polymer Chemistry, in press.
[8] Yenice Z, Tasdelen MA, Oral A, Guler C, Yagci Y. Journal of Polymer Science, Part A Polymer Chemistry 2009;47(8):2190–7.
[9] Choi KY, Kwag BG, Park SY, Cheong CH. 2009.
[10] Kolb HC, Finn MG, Sharpless KB. Angewandte Chemie – International Edition 2001;40(11):2004–21.
[11] Rostovtsev VV, Green LG, Fokin VV, Sharpless KB. Angewandte Chemie – International Edition 2002;41(14):2596–9.
[12] Tornoe CW, Christensen C, Meldal M. Journal of Organic Chemistry 2002;67(9):3057–64.
[13] Lutz JF. Angewandte Chemie – International Edition 2007;46(7):1018–25.
[14] Fournier D, Hoogenboom R, Schubert US. Chemical Society Reviews 2007;36(8):1369–80.
[15] Hawker CJ, Wooley KL. Science 2005;309(5738):1200–5.
[16] Binder WH, Sachsenhofer R. Macromolecular Rapid Communications 2008;29(12–13):952–81.
[17] Devaraj NK, Collman JP. Qsar & Combinatorial Science 2007;26(11–12):1253–60.
[18] Gil MV, Arevalo MJ, Lopez O. Synthesis-Stuttgart 2007;(11)::1589–620.
[19] Golas PL, Matyjaszewski K. Qsar & Combinatorial Science 2007;26(11–12):1116–34.
[20] Moses JE, Moorhouse AD. Chemical Society Reviews 2007;36(8):1249–62.
[21] Wu P, Fokin VV. Aldrichimica Acta 2007;40(1):7–17.
[22] Yagci Y, Tasdelen MA. Progress in Polymer Science 2006;31(12):1133–70.
[23] Evans RA. Australian Journal of Chemistry 2007;60(6):384–95.
[24] Fleming DA, Thode CJ, Williams ME. Chemistry of Materials 2006;18(9):2327–34.
[25] Binder WH, Sachsenhofer R, Straif CJ, Zirbs R. Journal of Materials Chemistry 2007;17(20):2125–32.
[26] Ranjan R, Brittain WJ. Macromolecules 2007;40(17):6217–23.
[27] Tasdelen MA, Van Camp W, Goethals E, Dubois P, Du Prez F, and Yagci Y. et-al 2008;41(16):6035–40.
[28] Voggu R, Suguna P, Chandrasekaran S, Rao CNR. Chemical Physics Letters 2007;443(1–3):118–21.
[29] Liu QC, Chen YM. Journal of Polymer Science, Part A: Polymer Chemistry 2006;44(20):6103–13.
[30] Su SP, Jiang DD, Wilkie CA. Polymers for Advanced Technologies 2004;15(5):225–31.
[31] Sen S, Memesa M, Nugay N, Nugay T. Polymer International 2006;55(2):216–21.
[32] Zhu J, Uhl FM, Morgan AB, Wilkie CA. Chemistry of Materials 2001;13(12):4649–54.
[33] Zhu J, Morgan AB, Lamelas FJ, Wilkie CA. Chemistry of Materials 2001;13(10):3774–80.
[34] Zhu J, Start P, Mauritz KA, Wilkie CA. Polymer Degradation and Stability 2002;77(2):253–8.
[35] Zeng CC, Lee LJ. Macromolecules 2001;34(12):4098–103.
[36] Laus M, Camerani M, Lelli M, Sparnacci K, Sandrolini F, Francescangeli O. Journal of Materials Science 1998;33(11):2883–8.
[37] Landrya V, Riedl B, Blanchet P. Progress in Organic Coatings 2008;62(4):400–8.
[38] Hirata T, Kashiwagi T, Brown JE. Macromolecules 1985;18(7):1410–8.
[39] Hwu J, Jiang GJ, Gao ZM, Xie W, Pan WP. Journal of Applied Polymer Science 2002;83(8):1702–10.
[40] Meneghetti P, Qutubuddin S. Langmuir 2004;20(8):3424–30.
[41] Xu YJ, Brittain WJ, Xue CC, Eby RK. Polymer 2004;45(11):3735–46.
[42] Shen ZQ, Simon GP, Cheng YB. Journal of Applied Polymer Science 2004;92(4):2101–15.
[43] Gao Z, Xie W, Hwu JM, Wells L, Pan WP. Journal of Thermal Analysis and Calorimetry 2001;64(2):467–75.